Influence of Road Surface Microtexture on Thin Water Film Traction

Yannick Beautru, Malal Kane, Minh Tan Do, Véronique Cerezo

Influence of Road Surface Microtexture on Thin Water Film Traction

Y. Beautru, M. Kane, M.-T. Do
LUNAM Université, Ifsttar, Bouguenais, France

V. Cerezo
Cete of Lyon, Department Laboratory of Lyon, Bron, France

ABSTRACT: This paper deals with the contribution of road surface microtexture to the relationship between tire/road friction and water depth. The main objectives are the estimation of local water depths trapped at the tire/road interface and the definition of a critical water depth which can be used for driver assistance and information systems. Tests are performed in laboratory. Specimens are slabs made of asphalt concrete and mosaics composed of coarse aggregates. The aggregate mosaics are sandblasted to simulate different microtexture levels. Friction is measured by the Dynamic Friction Tester (DFT) machine at various speeds ranging between 20km/h and 80km/h. Microtexture profiles are measured by laser sensors. It was found that the friction-water depth curves have an inverse-S shape and present an initial constant-friction part before decreasing to a minimum value. The critical water depth, defined as the water depth above which the friction coefficient collapses significantly, is determined from observed friction-water depth curves. Thickness of the water film trapped between the surface aggregate summits and device measuring pad/tire tread is estimated from contact models using surface texture profiles. The order of magnitude corroborates values found in the literature. Relationship between the local water depth, taking into account the tire/road contact conditions, and the global one, as measured by most sensors, is presented. Influence of surface microtexture is discussed in terms of exerted pressure to break through the water film.

1 INTRODUCTION

It is well known that the tire/road friction decreases when the road surface is wet. Moore (1975) for example showed that the water acts as a lubricant and reduces the fraction of the tire/road contact area where friction forces are generated. Despite this widely accepted explanation, few works have dealt with the relationship between the water depth and the tire/road friction, mostly when the water film is very thin (< 1mm). This situation occurs after rainfalls or during drizzles where the road surface has a damp aspect and provides a safety feeling. Delanne et al. (2006) showed that the speed adaptation on “just wet” roads is not enough compared with the friction loss due to water. This incompatibility explains why accident records are generally high after rainfalls. The tire/road friction loss on damp road surfaces is sometime referred to as “viscoplaning” in order to emphasize the viscous effect of thin water depths.

Moore (1975) also explained that only the road surface microtexture (surface asperities less than 0.2 mm in height and 0.5 mm in width) is capable of mitigating the viscoplaning. This author said that both asperity height and shape are important: the asperity height prevents asperity summits to be masked by the water film, whereas the asperity sharpness provides enough pressure to break through the water film. Pressures exerted by known geometrical shapes like spheres or cones are provided. Water thicknesses of tenth to hundredth of millimeter are mentioned.

Works by Moore (1975) or other authors like Savkoor (1990) have highlighted the role of road surface microtexture. However, more knowledge is still needed regarding the influence of

microtexture on thin water film traction. Within the frame of the European project SKIDSAFE (7th Framework Program) dedicated to the modelling of tire/road friction, Ifsttar has initiated a research aiming at developing a model predicting the onset of visco- and hydroplaning from the knowledge of road materials, tire characteristics and tire/road contact conditions (speed, wheel slip, water depth, etc.). The work presented in this paper is part of the Ph.D. of the first author focusing on the viscoplaning aspect. It is composed of three parts:

- in the first part, friction tests at different water depths are presented;
- in the second part, the shape of the friction-water depth plot is presented. Definition of a critical water depth is derived;
- in the third part, the influence of microtexture on both the friction-water depth plot and the critical water depth is analyzed.

2 FRICTION TESTS

2.1 *Friction devices*

Friction tests are performed in laboratory by means of the Dynamic Friction Tester (DFT). The machine is composed of a measuring unit (Fig. 1) and a control unit. The measuring unit consists of a horizontal fly wheel and disc which are driven by a motor. Three rubber sliders are attached to the disc by leaf springs. They are pressed on the test surface by the weight of the device and are loaded to 11.8 N each.

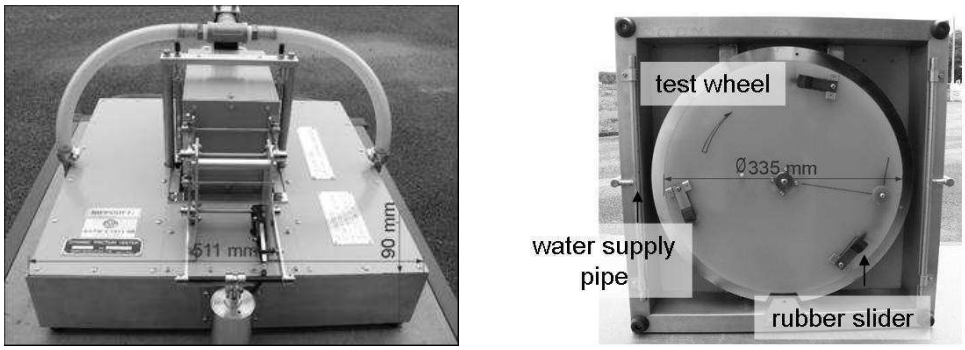

Figure 1. DFT machine.

2.2 *Specimens*

Specimens are 520 mm × 375 mm × 30 mm slabs. Four slabs are produced in laboratory: a very thin asphalt concrete (VTAC) 0/6 (the numbers indicate the size range, in millimeter, of coarse aggregates); a semi-coarse asphalt concrete (SCAC) 0/6; a sand asphalt and a mosaic composed of river coarse aggregates. Moreover, to study the effect of surface microtexture, the aggregate mosaic is sandblasted using 590µm corundum particles to simulate a microtextured surface. Actually, the sandblasting roughens the aggregate surface and, by consequent, modifies only the surface microtexture. VTAC and SCAC are representative of asphalt formulations used for main and secondary roads in France. The mosaic is made by placing coarse aggregates in a mold (Fig. 2a) then covering the bottom with sand and resin.

a) 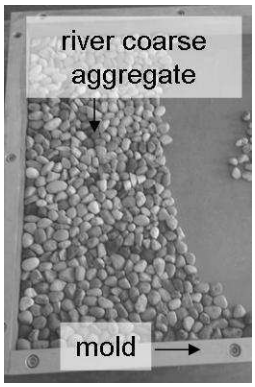

b) 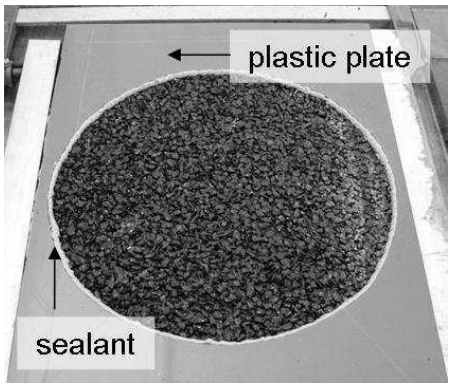

Figure 2. Laboratory specimens (a: coarse aggregate mosaic; b: asphalt slab).

2.3 *Test procedure*

The wetted surface is a circle of 345 mm of diameter carved in a plastic plate affixed to the specimen slab (Figure 2b). To avoid water from flowing from the test area, the edge of the circle is filled with a sealant, and the slab is covered, except on its upper face, by a waterproof sheet.

A spray is used to wet the surface. The amount of water sprayed on the test surface is known by weighing the spray before and after each friction measurement. Dividing the volume of water by the wetted area, an average water depth can be calculated. This water depth is called the "initial equivalent water depth" as it is the thickness of the water film before the friction test is performed. This wetting protocol enables the study of very thin water depths (few tenths of millimeters) for which no current sensor can measure.

For each friction test, new sliders are used to ensure that slider wear does not affect results. The test surface is leveled and free of any contamination. The DFT is placed above the slab using visual markers to ensure that it is always placed at the same location. Compared with the ASTM standard (2009), the test procedure is modified to study the influence of water depth on friction coefficient. Actually, the machine is programmed to run tests with no water from the supply unit; water is added uniquely by the spray. After a first measurement performed on a perfectly dry surface, the following procedure is repeated 12 times:

- wetting of the slab surface by nine sprayings (≈ 6 g of water in total);
- friction measurement;
- weighing of the spray.

At the end of the procedure, test using the standard procedure for the DFT is performed.

3 FRICTION/WATER DEPTH RELATIONSHIP

3.1 *Shape of the friction/water depth curve*

Example of friction/water depth plot is shown in the figure 3. The friction coefficient obtained by applying the ASTM standard (2009) is also shown (dotted line). It can be observed a three-phase variation:

- in phase 1, friction decreases from the "dry" value to a stable level;
- in phase 2, friction decreases rapidly;
- in phase 3, friction stabilizes at a "residual" level.

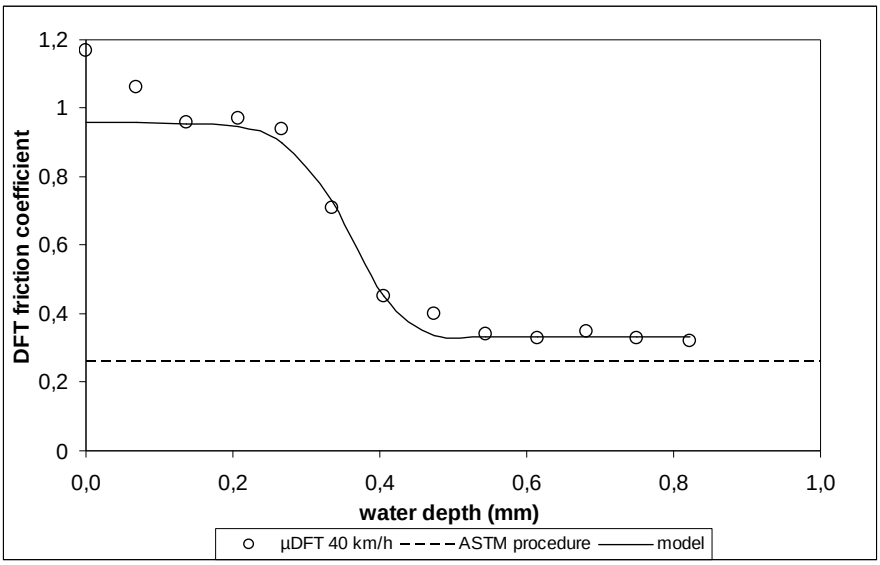

Figure 3. Variation of friction coefficient versus water depth.

The observed shape is different from that found in previous works where an exponential variation of friction with water depth is presented (Veith 1983, Kulakowski & Harwood 1990). The difference between figure 3 and published results can be attributed to the water quantity sprayed on the dry test surface to obtain the first wet state. If too much water is sprayed, the transition from "dry" to "wet" can be missed. Figure 3 also shows that the DFT friction coefficient measured by the ASTM procedure represents the lowest friction value that can be expected.

A mathematical model was developed to fit the shape of the friction/water depth curve derived from our experiments:

$$\mu = \Delta\mu \cdot e^{\left(-\frac{h}{h_0}\right)^{\alpha}} + \mu_F \qquad (1)$$

where μ = friction coefficient; h = water depth; μ_F = final friction coefficient; $\Delta\mu$ = difference between $\mu(0)$ (μ at h = 0) and μ_F; and h_0, α = constants.

The model (1) is similar to that proposed by Kulakowski & Harwood (1990) but can simulate other shapes than the exponential one. Actually, if $\alpha = 1$, an exponential variation can be found. For $\alpha \neq 1$, other shapes can be found. The continuous line in figure 3 shows how the model (1) fits experimental data.

3.2 *Critical water depth*

In the context of warning or driver assistance on wet roads, people look for a critical water depth, which can be measured or estimated in real time, above which something must be done. Based on the shape of the friction/water depth curve, it appears that the most critical phase is the transition from phase 1 to phase 2, where friction can drop drastically even if the road surface still displays an apparent "safe" aspect.

Dividing the friction/water depth curve into three parts corresponding respectively to the three variation phases, each part of the friction-water depth curve can be linearized as shown in the figure 4: a horizontal line to represent phase 1 (the decrease from the dry state value is neglected), a sloped line to represent phase 2, and again a horizontal line to represent phase 3. The critical water depth is then defined as the amount of water obtained at the intersection between phases 1 and 2 lines (arrow in figure 4). From this point, a small additional amount of water is sufficient to degrade significantly the friction coefficient. Within the frame of our experiments, critical water depths lower than 1 mm were found (0,28 mm in figure 4). Such

critical water depths can also determine the onset of viscoplaning as discussed in the introduction.

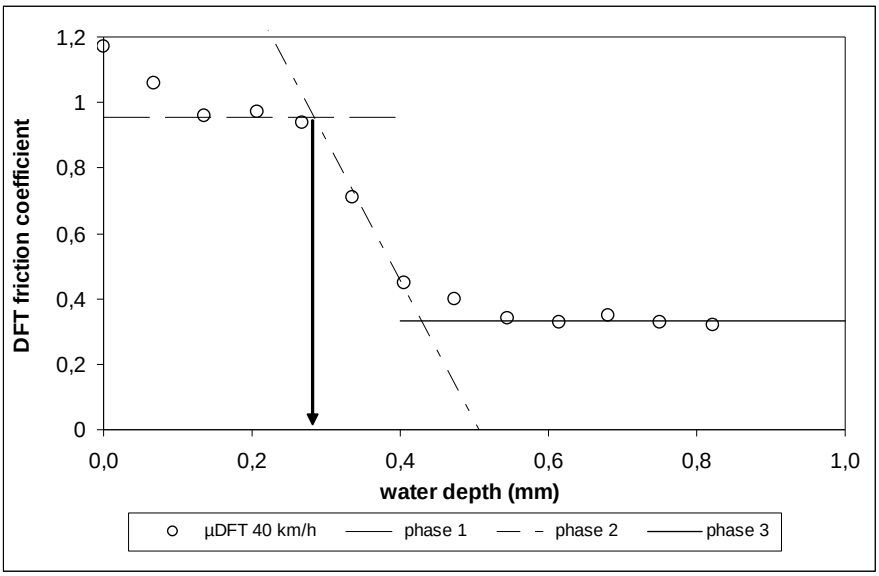

Figure 4. Definition of critical water depth.

4 INFLUENCE OF THE SURFACE MICROTEXTURE

4.1 *Microtexture and friction/water depth curve*

The influence of the surface microtexture can be assessed by comparison of results obtained from the aggregate mosaic respectively before and after sandblasting. Indeed, river aggregates are naturally smooth; they are roughened by sandblasting. Any difference between before- and after-sandblasting mosaics can then be attributed to the aggregate microtexture.

Figure 5 shows that when the surface is dry, the mosaic before sandblasting (called “smooth”) exhibits higher friction value than the sandblasted one. This is due to the fact that dry friction depends on available contact area, which is larger on smooth surfaces. However, the friction coefficient of the smooth mosaic drops rapidly as soon as the surface is wetted. In contrast, the sandblasted mosaic displays a more stable variation of the friction coefficient until a water depth of 0.3 mm is reached. Also, it can be seen that, even if both surfaces experience friction decrease with water depth, the sandblasted curve is always above the smooth curve. These observations corroborate those made by Moore (1975) on smooth and roughened spheres. The progress made in the present study is that observations are now made on surfaces composed of actual aggregates and an order of magnitude of the critical water depth can be derived.

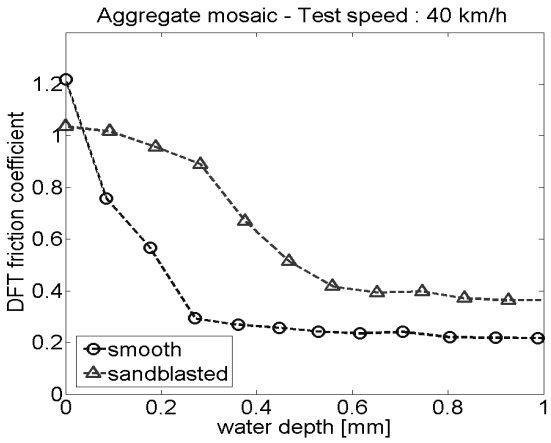

Figure 5. Influence of surface microtexture on friction/water depth curve.

Figure 5 clearly highlights the role of the surface microtexture to mitigate the risk of a brutal degradation of wet pavement skid-resistance while maintaining a high friction level. When the surface is wetted, asperities, mainly sharp ones, are needed to squeeze out the water film. Otherwise, as it happened with the smooth mosaic, water, even at very thin thicknesses, can penetrate very quickly in the tire/road contact area and causes contact loss between the tire and the road.

The above explanation is satisfactory at a qualitative level. Quantitative information is however needed to understand how the geometry of microtexture asperities contribute to the water evacuation and the friction generation. Visual observations would be the best first step towards this understanding. However, no current system can "see" what is happening at an asperity summit; modeling constitutes then a good alternative. In the following sections, attempts are made to model the friction forces generated between a rubber pad (representing a tire tread pad) sliding on a microtexture profile while this profile is masked progressively by water.

4.2 *Modeling of the contribution of microtexture*

The model considers a rubber slider moving over a symmetrical asperity with an angle 2α at the summit (Fig. 6). Considering the equilibrium of the slider on respectively the ascending and descending faces of the asperity, the following formulae can be written (Do 2004):

$$F_{xa} = \frac{F_{za}\left(\cos\alpha + \mu_0 \sin\alpha\right)}{\sin\alpha - \mu_0 \cos\alpha} \tag{2}$$

$$F_{xd} = \frac{F_{zd}\left(\mu_0 \sin\alpha - \cos\alpha\right)}{\sin\alpha + \mu_0 \cos\alpha} \tag{3}$$

$$\mu = \frac{F_x}{F_z} = \frac{F_{xa} + F_{xd}}{F_z} = h\frac{\cos\alpha + \mu_0 \sin\alpha}{\sin\alpha - \mu_0 \cos\alpha} - (1-h)\frac{\mu_0 \sin\alpha - \cos\alpha}{\sin\alpha + \mu_0 \cos\alpha} \tag{4}$$

$$h = \frac{F_{za}}{F_z} \tag{5}$$

where F_x, F_z = horizontal and vertical forces respectively; F_{xa}, F_{xd} = components of F_x on ascending and descending faces respectively; F_{za}, F_{zd} = components of F_z on ascending and descending faces respectively; μ = friction coefficient; 2α = angle at the asperity summit; h = factor defining the distribution of F_z on the asperity; and μ_0 = friction coefficient encountered

by the slider on the asperity ascending and descending faces (we assume both faces have the same friction coefficient).

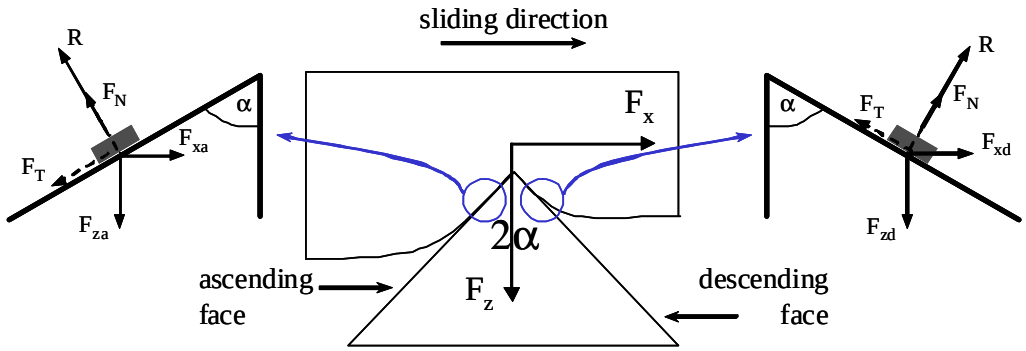

Figure 6. Rubber slider moving over a symmetrical asperity.

The "h" factor is equal to 0.5 if the slider is elastic (symmetrical deformation). For rubber, for which the viscoelastic behavior creates an asymmetrical deformation, h depends on its properties; a value of h = 0.83 was adopted in (Do 2004) and is used for the present study.

Microtexture profiles are measured on the mosaic aggregates by means of laser sensor. Profiles are sampled every 0.01 mm. Example of measured profile is shown in figure 7. For the two mosaics, values of the height root-mean-square (RMS) (also known as R_q in surface roughness language) are 6.9 µm and 17.9 µm for respectively the smooth and sandblasted mosaics.

Profile summits and valleys are first detected as respectively local maxima and minima. Each asperity composed of a summit and its two neighbor valleys is then considered and the 2α angle calculated.

The influence of water is reflected through the masking of the asperity summits and, by consequence, the friction force. Actually, the angle α taken into account in formulae (2)(3)(4) is the average of angles α determined for all profile asperities. As those asperities are progressively submerged by water, it is thought that the resulting α value should be water-depth dependent (only asperities "seen" by the slider are taken into consideration). The masking mechanism is quite simple at this stage: the water film is represented by a horizontal line (dotted line in figure 7) moving upward as the water thickness increases. The water depth is the height difference between the dotted line and the zero line, which also represents the mean profile line; the water depth represented in figure 7 is 15 µm. The mean profile line also represents the aggregate summit where microtexture profiles are measured.

Friction force calculation takes into account the fact that, as the water depth increases, the vertical force is supported by both the water film (where asperities are submerged) and the profile asperities. This consideration prevents the fact that, as the number of asperities seen by the rubber slider decreases, friction force can be abnormally high if the whole vertical force is supported only by the few remaining asperities. The friction coefficient μ_0 is often considered as the adhesion – bonding – component of friction. Kummer & Meyer (1966) said that adhesion can also be considered as the micro-hysteresis – deformation – component of friction. The "micro" term can be interpreted as what cannot be seen. As the microtexture profiles are sampled every 0.01 mm, we assume that μ_0 represents friction forces generated by asperities smaller than 10 µm in width. Previous studies (Do 2004) showed that the contribution of asperities less than 10 µm is roughly independent of the aggregate microtexture; a common value of 0.3 was found and is adopted as μ_0 for the present study.

To summarize, the model calculates friction forces from an indicator of microtexture sharpness (angle α), and the masking effect due to water takes into account microtexture height.

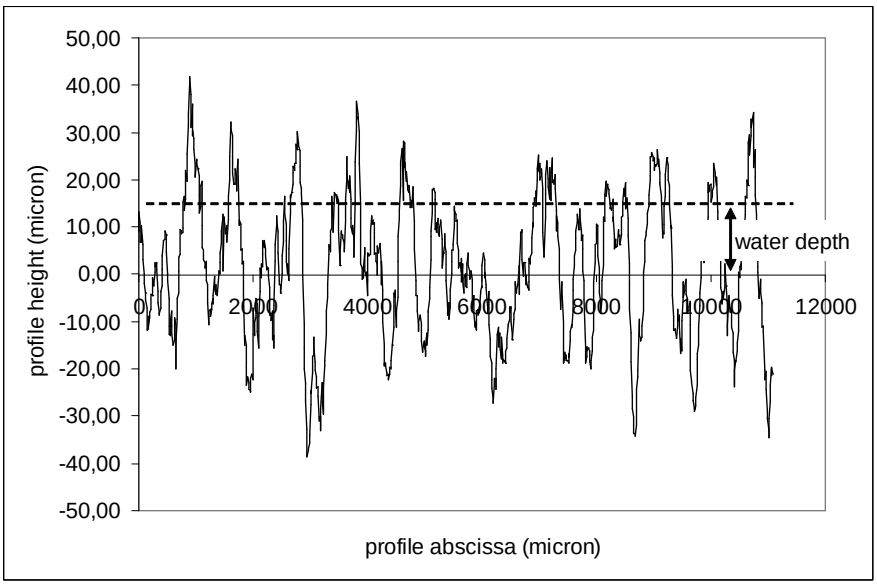

Figure 7. Example of microtexture profile and illustration of the masking effect of water.

The variation of friction coefficient with water depth as predicted by the model is shown in figure 8. The order of magnitude of water depths is much lower (ten times less) than that observed in previous graphs (Figs 3, 5). It should be noted that the water depth of figures 3 and 5 (initial equivalent water depth, see 2.3) is due to water poured on the surface before friction measurements, whereas the water depth of figure 8 is due to water trapped between the tire tread and the road surface asperity summits. According to many authors (Moore 1975, Savkoor 1990), the thickness of the trapped water film can be just a few microns.

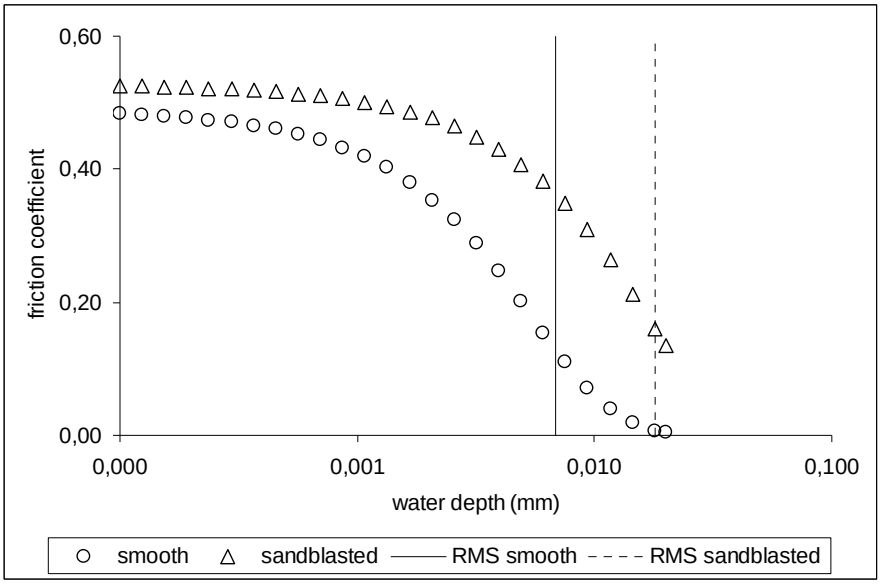

Figure 8. Predicted friction/water depth curve.

The curves in figure 8 confirms the observation made from figure 5: i) the sandblasted mosaic shows a friction/water depth variation more stable than the smooth mosaic, and ii) the sandblasted-mosaic curve is above the smooth-mosaic curve.

From theoretical results, we can explain the observations in figure 5 as following:

- the role of microtexture asperity height explains the friction/water depth variation. During phase 1 (see 3.1 for definition), a stable variation reflects the fact that asperity heights are enough to maintain the friction level. Previous papers (Savkoor 1990, Schipper 1990) mentioned that the profile RMS is a good indicator to assess the beginning of the delubrication process. Reporting respective values of RMS of smooth and sandblasted mosaics in figure 8, it can be seen that they are located roughly at the transition between phase 2 and phase 3. Knowing that phase 3 is referred to as "hydrodynamic lubrication" regime (Schipper 1990), where two solids (the tire and the road surface in the present study) previously in contact are separated by a continuous lubricant film, our observation corroborates those made in previous works on other types of contact.
- for microtexture asperities not submerged by the water film, their sharpness helps to generate friction forces. There is a state where the number of asperities is not high enough and friction coefficient starts to collapse; this location was used to define the critical water depth (3.2).

The short theoretical study conducted does not intend, at this stage, to reproduce experimental observations (even if it constitutes the very first stage towards this objective). However, it helps us better understand how microtexture contributes to thin film traction. Literature is abounded with explanations about the role of microtexture descriptors like their height, shape and density. Our study has made some progress by showing quantitatively the respective roles of microtexture height and shape on the way friction varies with water depth.

5 CONCLUSIONS

In this study, we are focused on the relationship between tire/wet road friction and road wetness. Thin water films (< 1 mm) are of interest because of the damp aspect that conveys a safety feeling to drivers and induces accidents. Laboratory tests are performed. Friction is measured for different water quantities poured on the test surface. Equivalent water depth is derived from the poured water volume. The friction/water depth plot shows a three-phase variation: 1) the friction coefficient remains at a level near the dry-surface one, then it collapses at the so-called critical water depth before reaching a residual level. Comparison between surfaces with similar macrotexture shows the importance of microtexture to maintain the phase 1 as long as possible and to preserve an acceptable friction level when the water depth increases. A simple friction model was used to get better understanding about the influence of microtexture: it shows that microtexture height is necessary to prevent (or mitigate) friction to collapse, whereas microtexture sharpness helps to generate friction forces.

6 REFERENCES

ASTM E1911 2009. Standard Test Method for Measuring Paved Surface Frictional Properties Using the Dynamic Friction Tester. ASTM.

Do, M.T. 2004. *Contribution of road-texture scales to pavement skid-resistance (in French, summary in English).* Report n° LPC-ER-CR 04-35. Paris: LCPC.

Ford, I.J. 1993. Roughness Effect on Friction for Multi-Asperity Contact Between Surfaces. *Journal of Physics D: Applied Physics* 26: 2219-2225.

Kulakowski, B.T. & Harwood DW. 1990. Effect of Water-Film Thickness on Tire-Pavement Friction. In W.E. Meyer & J.Reichter (eds), *Surface Characteristics of Roadways: International Research and Technologies, ASTM STP 1031:* 50-60. Philadelphia: ASTM.

Kummer, H.W., Meyer, W.E. 1966. New Theory Permits Better Frictional Coupling between Tire and Road. *Proceedings of the 11th International FISITA Congress:* 3-37.

Moore, D.F. 1975. *The Friction of Pneumatic Tyres.* Elsevier Scientific Publishing Company.

Savkoor, A.R. 1990. Tribology of Tyre Traction on Dry and Wet Roads. *Proceedings of the 17th Leeds – Lyon Symposium on Tribology:* 213-228.

Schipper, D.J. 1990. *Transitions in the Lubrication of Concentrated Contacts*. PhD Thesis. University of Twente.

Veith, A.G. 1983. Tires – Roads – Rainfall – Vehicles: The Traction Connection. In W.E. Meyer & J.Reichter (eds), *Frictional Interaction of Tire and Pavement, ASTM STP 793*: 3-40. Philadelphia: ASTM.